Materials Research Bulletin 82 (2016) 26–30

Contents lists available at ScienceDirect

Materials Research Bulletin

journal homepage: www.elsevier.com/locate/matresbu

Nondegenerate n-type doping phenomenon on molybdenum disulfide (MoS_2) by zinc oxide (ZnO)

Dong-Ho Kang[a,1], Seong-Taek Hong[a,1], Aely Oh[a], Seung-Hwan Kim[b], Hyun-Yong Yu[b,**], Jin-Hong Park[a,*]

[a] School of Electronic and Electrical Engineering, Sungkyunkwan University, Suwon 440-746, South Korea
[b] School of Electrical Engineering, Korea University, Seoul 136-701, South Korea

ARTICLE INFO

Article history:
Received 2 September 2015
Received in revised form 13 February 2016
Accepted 19 February 2016
Available online 23 February 2016

Keywords:
A. Semiconductor
A. Electronic materials
A. Layered compounds
D. Electrical properties
D. Electronic structure

ABSTRACT

In this paper, we have demonstrated nondegenerate n-type doping phenomenon of MoS_2 by ZnO. The ZnO doping effects were systematically investigated by Raman spectroscopy and electrical/optical measurements (I_D–V_G with/without exposure to 520, 655, 785, and 850 nm laser sources). The ZnO doping improved the performance parameters of MoS_2-based electronics ($I_{on}\uparrow$, $\mu_{FE}\uparrow$, $n\uparrow$) owing to reduction of the effective barrier height between the source and the MoS_2 channel. We also monitored the effects of ZnO doping during exposure to air; reduction in ΔV_{TH} of about 75% was observed after 156 h. In addition, the optoelectronic performance of the MoS_2 photodetector was enhanced due to the reduction of the recombination rate of photogenerated carriers caused by ZnO doping. In our results, the highest photoresponsivity (about 3.18×10^3 A/W) and detectivity (5.94×10^{12} Jones) of the ZnO-doped photodetector were observed for 520 nm laser exposure.

1. Introduction

Transition metal dichalcogenides (TMDs) with two-dimensional (2D) semiconducting layered structure, such as molybdenum disulfide (MoS_2) and tungsten diselenide (WSe_2), have been considered to be extremely promising materials for future transparent, flexible and wearable electronic/optoelectronic devices because of their exceptional electrical [1–3], optoelectronic [4] and mechanical properties [5]. Because of the excellent thickness scalability of TMDs as an atomic monolayer and van der Waals epitaxial structure without dangling bonds, TMD-based electronic devices have immunity to the short-channel effects; thus, they have been contemplated for future high-performance nanoelectronic applications [2,6]. In addition, TMD materials are expected to be suitable for high-performance optoelectronic devices (i.e., photodetectors and solar cells) because of their tunable band gap (between 1.2 and 1.8 eV, depending on layer thickness) and extremely high quantum efficiency [7,8].

To further improve the performance of TMD-based electronic/optoelectronic devices, it is necessary to reduce the contact resistance of metal–semiconductor junctions and to lower the recombination rate of carriers. However, such improvements cannot be carried out by using the ion implantation technique on TMD material because of the crystal damage of the 2D structure. For these reasons, recent work has focused on the developing of less disruptive doping techniques for application to TMD devices. Recently, Fang et al. reported p- and n-type doping technique on TMD devices, which involved the use of NO_2 molecules and potassium, respectively [9,10]. However, both p- and n-doping techniques produced very high levels of doping, making the TMD channel layers near metallic. Thus, development of lighter doping techniques for use with TMD devices is crucial for the optimization of TMD-based electronics/optoelectronics. Lin et al. and Park et al. reported low-level doping techniques using Cs_2CO_3 ($\sim 1 \times 10^{11}$ cm^{-2} on MoS_2) and DNA/M-DNA ($\sim 6.4 \times 10^{10}$ cm^{-2} on MoS_2), respectively [11,12].

Here, we also reported the nondegenerate n-type doping technique on MoS_2 by zinc oxide (ZnO) film coating. The negative polar surface of the ZnO film was expected to reduce the hole carrier density in the MoS_2 channel layer, thereby causing an n-doping effect. We investigated the ZnO doping effects on MoS_2 by Raman spectroscopy and electrical measurements (I_D–V_G and I_D–V_D). In addition, we also monitored the V_{TH} variations of ZnO-doped MoS_2 devices during 156 h of exposure to air. Finally, the

* Corresponding author at: Sungkyunkwan University, Natural Sciences Campus, Cheoncheon-dong, Jangan-gu, South Korea.
** Corresponding author.
E-mail addresses: jhpark9@skku.edu (J.-H. Park), yuhykr@korea.ac.kr (H.-Y. Yu).
[1] These authors contributed equally to this work.

http://dx.doi.org/10.1016/j.materresbull.2016.02.029
0025-5408/

effects of ZnO doping upon the photoresponsivity and detectivity performance of MoS_2-based optoelectronic devices were observed by means of optical measurements performed under exposure to laser sources of wavelengths 520, 655, 785, and 850 nm.

2. Experiments

For the fabrication of back-gated MoS_2 devices (transistors and photodetectors), source/drain electrode regions were patterned (channel length and width are 5 um) on $MoS_2/SiO_2/Si$ samples by optical lithography, followed by Ti (10 nm) and Au (50 nm) deposition via e-beam evaporation. ZnO solutions were prepared by dissolving 1.1 g of zinc acetate dihydrate [$Zn(CH_3COO)_2{\cdot}2H_2O$] and 0.3 mL of monoethanolamine (MEA) in 8.96 mL of 2-methoxyethanol as the solute, stabilizer and solvent, respectively. The molar ratio of MEA to zinc acetate dihydrate was maintained at 1.0 and the concentration of zinc acetate dihydrate was 0.5 M. The solution was stirred at 60 °C for 2 h in air to obtain a transparent and homogeneous solution, followed by aging at room temperature for 5 days. For doping of MoS_2 devices, the ZnO solutions were dropped onto MoS_2 devices and spin coated at 3000 rpm for 15 s. Subsequently, the ZnO-doped MoS_2 devices were annealed by using a thermal furnace operated at 250 °C for 15 min in air ambient. The devices were electrically analyzed by using an HP4155A semiconductor parameter analyzer, and the carrier concentration (n), field-effect mobility (u_{FE}) and threshold voltage (V_{TH}) were calculated by using the current–voltage (I_D–V_G) data. To investigate the optoelectronic properties of the fabricated ZnO-doped MoS_2 devices, the I_D–V_G measurements were performed under both dark and illuminated conditions. Here, all drain currents (I_D) were normalized by channel width (W). The light sources were set up by using a dot laser of wavelength 520, 655, 785, and 850 nm and an optical power of 6 mW/cm^2. Photoresponsivity (R) and detectivity (D*) were calculated by using the acquired I_D–V_G curves.

3. Results and discussion

To verify the doping effects of ZnO film on MoS_2 film, we performed Raman spectroscopy on ZnO-doped MoS_2 samples exfoliated on a SiO_2/Si substrate. Fig. 1a shows Raman spectra of undoped/ZnO-doped MoS_2 samples. In MoS_2 samples, the two conventional peaks (E^1_{2g} and A_{1g}) were observed at about 380 and 406 cm^{-1}, attributed to the in-plane (E^1_{2g} peak) and out-of-plane (A_{1g} peak) vibrations of MoS_2 [13]. We then extracted E^1_{2g} and A_{1g} peak positions for each undoped/doped MoS_2 sample (Fig. 1b). In the case of control samples of undoped MoS_2, the E^1_{2g} and A_{1g} peak positions were located at 380–380.5 and 405.2–405.8 cm^{-1}, respectively. After ZnO doping, those two peaks were red-shifted (379.4–380.2 cm^{-1} for E^1_{2g} and 404.6–405.3 cm^{-1} for A_{1g}). These phenomena indicated that ZnO causes the softening of MoS_2 vibrational modes and consequently causes n-type doping effects in MoS_2 films [14]. The Raman shifts of the two peaks were 0.3–0.6 cm^{-1}, indicating that the ZnO treatment produced low levels of doping, as desired.

To confirm the doping effects of ZnO on MoS_2 once again, we fabricated MoS_2-based transistors and performed the electrical measurement (I_D–V_G). Fig. 2a shows the three-dimensional schematic illustrations of ZnO-doped MoS_2 back-gated transistors and an energy band diagram of the metal (Ti)-undoped/doped MoS_2 junctions. Because the ZnO crystal structure is asymmetric wurtzite, it has ionic and polar structures consisting of oxygen- and zinc-terminated surfaces [15]. From these effects, the hole carriers further accumulated at the interface between ZnO and MoS_2, thereby causing the n-doping phenomenon on the MoS_2 channel layer. As shown in Fig. 2a, these negative polar surface of ZnO was expected to be reduced the effective barrier height of the Ti-MoS_2 junction by shifting down of the MoS_2 energy band at the source–MoS_2 junction (Schottky barrier lowering effect: $\Phi_{Control,eff} > \Phi_{ZnO,eff}$), eventually influencing the tunneling of electron carriers from the source metal to MoS_2. This ZnO doping mechanism is similar to that of self-assembled monolayer (SAM) [16,17] and DNA/M-DNA doping [12]. As a result, a negative shift in threshold voltage (V_{TH}) from −3.8 to −11.6 V and an on-current enhancement from 1.6×10^{-6} to 8.27×10^{-6} A/μm were observed in the ZnO-doped MoS_2 transistors (Fig. 2b). We then calculated field-effect mobility (μ_{FE}) and 2D sheet concentrations (n) of undoped/ZnO-doped MoS_2 devices for investigating the changes in electronic performance caused by ZnO doping. Here, the field-effect mobility and concentration were extracted by using the following equations: $\mu_{FE} = L/(WV_DC_{OX}) \times (\partial I_D/\partial V_G)$ and $n = I_DL/qW\mu V_D$, where q is the electron charge, L and W are the length and width of the channel, respectively, and C_{OX} is the gate oxide capacitance per unit area, $\varepsilon_{OX} \times \varepsilon_0/t_{OX}$. As shown in Fig. 2(c), the field-effect mobility value was increased from 12.8 to 29.3 cm^2/V-sec after ZnO doping, indicating that the ZnO doping improved the field-effect mobility by increasing the carrier injection probability. This mobility improvement phenomenon by doping has also been reported

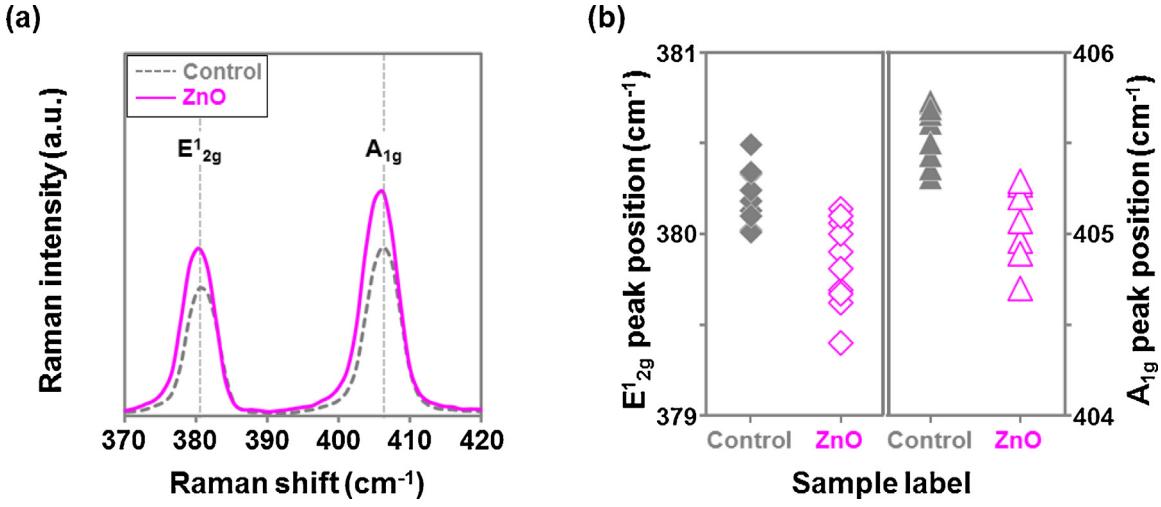

Fig. 1. (a) Raman spectra of undoped/ZnO-doped MoS_2 films. (b) Extracted E^1_{2g} and A_{1g} peak positions of undoped/ZnO-doped MoS_2 films.